Biochemical Pharmacology 245 (2026) 117665

Contents lists available at ScienceDirect

Biochemical Pharmacology

journal homepage: www.elsevier.com/locate/biochempharm

Probenecid Suppresses Migration, invasion and angiogenesis in hepatocellular carcinoma by modulating purinergic signaling and p38 MAPK pathway

Ilenia Matera [a], Alessandro Pistone [a], Maria Antonietta Castiglione Morelli [a], Faustino Bisaccia [b], Angela Ostuni [a,*]

[a] Department of Basic and Applied Sciences, University of Basilicata, Via dell'Ateneo Lucano 10, 85100 Potenza, Italy
[b] Department of Health Science, University of Basilicata, Via dell'Ateneo Lucano 10, 85100 Potenza, Italy

ARTICLE INFO

Keywords:
Probenecid
HepG2 cells
Purinergic signaling
EMT
Matrix metalloproteinases
Angiogenesis
p38 MAPK pathway

ABSTRACT

Probenecid (PBN) is a well-established therapeutic agent traditionally used to treat gout and to regulate renal excretion by inhibiting ATP-related membrane transporters. While these properties are well documented, their potential relevance in cancer biology remains largely unexplored. Given the critical role of extracellular ATP and purinergic signaling in tumor progression, we hypothesized that PBN might exert antitumor effects by interfering with this pathway. In this study, we investigated the anticancer activity of PBN in HepG2 human hepatocellular carcinoma cells and in an orthotopic mouse model. PBN enhanced cell adhesion and reduced migration and invasion, effects associated with altered integrin expression, selective inhibition of matrix metalloproteinase (MMP) activity, modulation of epithelial–mesenchymal transition (EMT) markers and reduced activation of the p38 MAPK pathway. In vivo, PBN suppressed tumor growth and reduced circulating vascular endothelial growth factor (VEGF) levels, indicating impaired angiogenesis.

Altogether, these findings indicate that PBN may represent a promising candidate for drug repurposing in hepatocellular carcinoma. By modulating purinergic signaling and selectively inhibiting p38 MAPK, PBN appears to limit tumor invasiveness and angiogenesis, supporting its potential relevance for further preclinical and clinical investigation.

1. Introduction

Hepatocellular carcinoma (HCC) is one of the leading causes of cancer-related mortality worldwide, often characterized by aggressive progression and poor prognosis. Despite advances in surgical and systemic therapies, prognosis remains poor for many patients, emphasizing the need for new therapeutic strategies that target the molecular mechanisms of tumor growth and dissemination [1]. Drug repurposing has recently gained attention as a promising approach in oncology. By identifying new applications for approved drugs, this strategy leverages established safety profiles, reduces development costs, and accelerates clinical translation [2,3].

Extracellular ATP plays a central role in tumor biology by promoting immune evasion, angiogenesis, proliferation and metastasis. In the tumor microenvironment, ATP is released by stressed, apoptotic or necrotic cells through transporters and channels such as ABC

Abbreviations: ADO, adenosine; ADORA, adenosine A2A receptor; AKT, protein kinase B; ATP, adenosine triphosphate; BLI, bioluminescence imaging; CD73, ecto-5′-nucleotidase; CDH1, cadherin 1 (E-cadherin); CDH2, cadherin 2 (N-cadherin); DMEM, Dulbecco's Modified Eagle Medium; DMSO, dimethyl sulfoxide; ECM, extracellular matrix; ELISA, enzyme-linked immunosorbent assay; EMT, epithelial–mesenchymal transition; ERK, extracellular signal-regulated kinase; FBS, fetal bovine serum; GAPDH, glyceraldehyde-3-phosphate dehydrogenase; HCC, hepatocellular carcinoma; HRP, horseradish peroxidase; IP, intraperitoneal; ITGA, integrin subunit alpha; ITGB, integrin subunit beta; MAPK, mitogen-activated protein kinase; MMP, matrix metalloproteinase; PBS, phosphate-buffered saline; PBN, probenecid; PI3K, phosphoinositide 3-kinase; SEM, standard error of the mean; SDS-PAGE, sodium dodecyl sulfate–polyacrylamide gel electrophoresis; VEGF, vascular endothelial growth factor; VIM, vimentin.

* Corresponding author.
E-mail addresses: ilenia.matera@unibas.it (I. Matera), alessandro.pistone@unibas.it (A. Pistone), maria.castiglione@unibas.it (M.A. Castiglione Morelli), faustino.bisaccia@unibas.it (F. Bisaccia), angela.ostuni@unibas.it (A. Ostuni).

https://doi.org/10.1016/j.bcp.2025.117665
Received 20 September 2025; Received in revised form 11 December 2025; Accepted 23 December 2025
Available online 24 December 2025

Table 1
List of primers used in this study.

Gene	Accession number	Forward primer	Reverse primer
β-actin	NM_001101.3	5′-CCTGGCACCCAGCACAAT-3′	5′-GCCGATCCACACGGAGTACT-3′
ADORA1	NM_000674.3	5′-CCACAGACCTACTTCCACACC-3′	5′-TACCGGAGAGGGATCTTGACC-3′
ADORA2A	NM_000675.6	5′- AACCTGCAGAACGTCACCAA −3′	5′- GTCACCAAGCCATTGTACCG −3′
ADORA2B	NM_000676.4	5′-GTCCGCTCAGGTATAAAAG-3′	5′-GAGTCAATCCGATGCCAAAG-3′
ADORA3	NM_000677.4	5′–GTCAGATACAAGAGGGTCAC-3′	5′-GTCAGTTTCATGTTCCAGCC-3′
CDH1	NM_001317184.2	5′-CTCCCTTCACAGCAGAACTAACAC-3′	5′-GTCCTCTTCTCCGCCTCCTTC-3′
CDH2	NM_001308176.2	5′-GGATCAAAGCCTGGAACATAT-3′	5′-TTGGAGCCTGAGACACGATT-3′
ITGA2	NM_002203.4	5′-AAATGATATTCTGATGCTGGG-3′	5′-CCAGCCTTTTCTAGTAGAGC-3′
ITGA6	NM_000210.4	5′-CTTAGGTTTTTCTTTGGACTCA-3′	5′-TCTCTTCAGCAAAACCACGG-3′
ITGB1	NM_000660.7	5′-CAGAATTGGATTTGGCTCATTT-3′	5′-AATGGGATAGTCTTCAGCTCTC-3′
P2RX7	NM_002562.6	5′-CCTTTGCAG GGGAACTCTT −3′	5′-TCTGAATTCCTTTGCTCTG −3′
P2RY1	NM_002563.5	5′-TGTGGTGGTGGCGATCTCC-3′	5′-TCGCAGGTACTCGTCTGAGG-3′
P2RY14	NM_001081455.2	5′-TCAGCATTGTGTTCTTTGGG-3′	5′-TGCTGTAACTCACTGACTGG-3′
P2RY2	NM_176072.3	5′-TGCCACCTG CCTTCTCACT-3′	5′- CTGGGAAATCTCAAGGACTG-3′
VIM	NM_003380.5	5′-ATGGACAGGTTATCAACGAAA-3′	5′-AAGTTTGGAAGAGGCAGAGA-3′

β-actin, Beta Actin; ADORA1, Adenosine A1 Receptor; ADORA2A, Adenosine A2A Receptor; ADORA2B, Adenosine A2B Receptor; ADORA3, Adenosine A3 Receptor; CDH1, Cadherin 1 (E-Cadherin); CDH2, Cadherin 2 (N-Cadherin); ITGA2, Integrin Subunit Alpha 2; ITGA6, Integrin Subunit Alpha 6; ITGB1, Integrin Subunit Beta 1; P2RX7, Purinergic Receptor P2X 7; P2RY1, Purinergic Receptor P2Y 1; P2RY2, Purinergic Receptor P2Y 2; P2RY14, Purinergic Receptor P2Y 14; VIM, Vimentin.

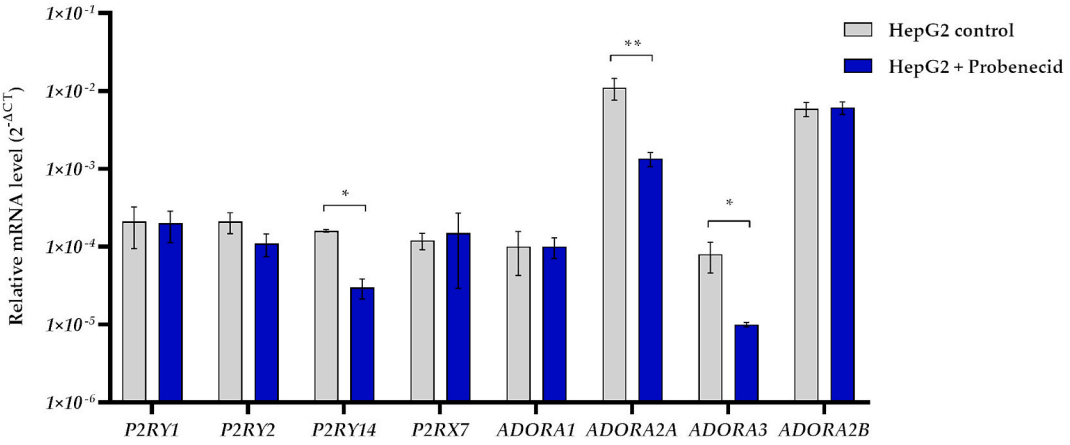

Fig. 1. Relative mRNA expression of key purinergic receptor genes in HepG2 cells. The mRNA levels of purinergic receptor genes in control and PBN-treated HepG2 cells were quantified by RT-qPCR, normalized to β-actin and expressed as $2^{-\Delta Ct}$. Data are presented as mean ± SEM from at least three independent experiments. Statistical analysis was conducted using Student's *t*-test; *p < 0.05, **p < 0.01.

transporters, pannexin-1 and connexins [4]. Once released, ATP and its metabolites activate purinergic receptors to regulate diverse signaling pathways [5]. Therefore, given this central role, targeting ATP-mediated signaling has emerged as a potential therapeutic strategy in cancer [6].

Probenecid (PBN) is a sulfonamide drug historically used for the treatment of gout, where it inhibits urate reuptake in renal tubules and facilitates urate excretion [7]. Beyond its classical pharmacological role, PBN acts as a broad-spectrum inhibitor of ATP-related transport mechanisms, including multidrug resistance proteins (MRPs/ABCC transporters) and pannexin-1 channels [8–11]. Through inhibition of these transporters, PBN has been proposed as a chemosensitizer capable of enhancing anticancer drug efficacy [12,13], while its ability to modulate extracellular ATP release influences purinergic signaling in the tumor microenvironment [5]. Recent studies have begun to elucidate the biological consequences of PBN-mediated modulation of purinergic pathways in hepatocellular carcinoma. PBN reduces extracellular ATP availability and regulates CD73 activity—the ectonucleotidase responsible for converting ATP into adenosine—in HepG2 cells [14,15]. In addition, PBN disrupts actin cytoskeleton organization, leading to loss of filopodia and reduced cell migration in HepG2 and in colon cancer cells [15,16]. Since ATP-dependent purinergic signaling orchestrates key tumor-related processes such as migration, invasion, and angiogenesis [5], these observations support the concept that PBN may attenuate malignant features of HCC and potentially other tumor types.

Although previous studies have suggested an anticancer potential for PBN, the mechanisms underlying its effects require clarification. This study therefore aimed to characterize the molecular basis of PBN action, using HepG2 cells as a well-established HCC model with a defined purinergic signaling background. By integrating *in vitro* and *in vivo* approaches, the present study provides evidence that PBN interferes with key steps of HCC progression, including epithelial-to-mesenchymal transition (EMT), invasion, and angiogenesis. Given its well-characterized pharmacokinetics and established clinical use, PBN emerges as a promising candidate for therapeutic repurposing through modulation of purinergic signaling.

2. Materials and methods

2.1. Cell culture and reagents

Human hepatocarcinoma cells (HepG2 cells; ATCC, Manassas, VA, USA) were cultured in Dulbecco's Modified Eagle's Medium (DMEM) (Thermo Fisher Scientific, Waltham, MA, USA), supplemented with 10 % fetal bovine serum (FBS; Thermo Fisher Scientific, Waltham, MA, USA), 2 mM L-glutamine, penicillin (100 U/mL)-streptomycin (100 μg/mL). Cells were maintained at 37 °C in a humidified 5 % CO_2 atmosphere and used within the sixth passage. PBN, ADO and SB203580 (Sigma, St. Louis, MO, USA) were dissolved in dimethyl sulfoxide (DMSO; Sigma-

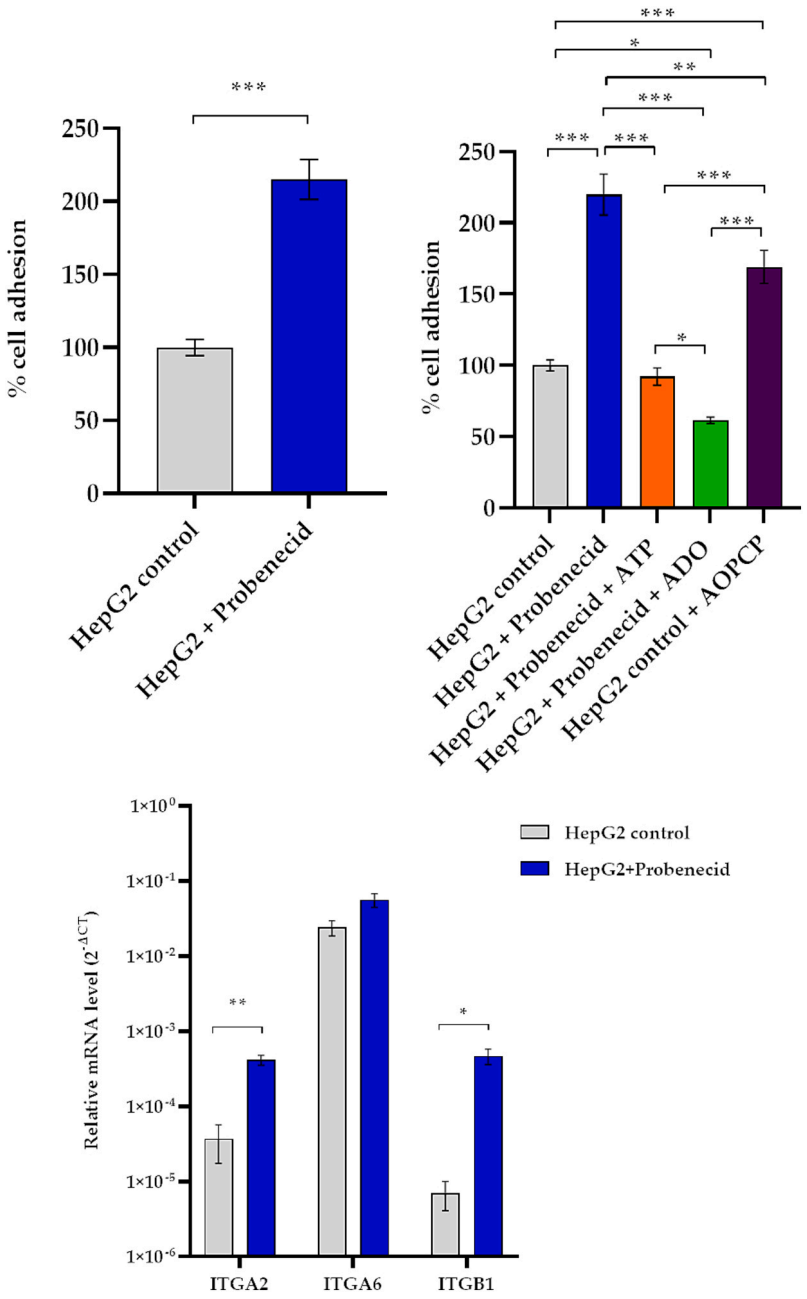

Fig. 2. Impact of Probenecid, ATP and ADO on HepG2 cell adhesion and ECM-related gene expression (a) Adhesion of HepG2 control and PBN-treated cells to Matrigel expressed as the percentage of adherent cells relative to the total population. (b) Effect of ATP and ADO on adhesion of PBN-treated HepG2 cells, quantified as a percentage of the total cell population. (c) Relative mRNA levels of ITGA2, ITGA6 and ITGB1 in control and PBN-treated HepG2 cells normalized to β-actin and expressed as $2^{-\Delta Ct}$. Data represent mean ± SEM from three independent experiments each with three biological replicates. Statistical analysis was performed using Student's *t*-test (A, C); *p < 0.05; **p < 0.01; ***p < 0.001 and one-way ANOVA with Holm-Sidak correction (B); *p < 0.05; ***p < 0.001.

Aldrich, St. Louis, MO, USA) to prepare stock solutions. Final DMSO concentrations in culture medium did not exceed 0.2 %. ATP was dissolved in sterile water.

2.2. Quantitative PCR (RT-qPCR)

Total RNA was isolated using the Quick-RNA™ MiniPrep kit (Zymo Research, Irvine, CA, USA), and purity and concentration were assessed via NanoDrop spectrophotometry. cDNA was synthesized using the High-Capacity cDNA Reverse Transcription Kit (Applied Biosystems, Waltham, MA, USA). Quantitative PCR was performed in triplicate using gene-specific primers (Table 1) and gene expression was calculated using the $2^{-\Delta CT}$ method, normalized to β-actin. All experiments were repeated independently at least three times.

2.3. Protein extraction and Western blotting

HepG2 cells were seeded at 6×10^5 cells/well in 6-well plates and incubated for 24 h to allow adhesion. Cells were then treated with 250 μM PBN, as previously established [17]. After treatment, cells were washed with PBS and lysed in RIPA buffer (0.1 % SDS, 1 % NP-40, 0.5 % sodium deoxycholate, pH 7.4) supplemented with protease and phosphatase inhibitors (Roche Diagnostics, Mannheim, Germany). Lysates were sonicated and centrifuged at 13,000 rpm for 10 min at 4 °C, and protein concentrations were measured using the Bradford Assay (Sigma-Aldrich, St. Louis, MO, USA). Equal amounts of protein were separated

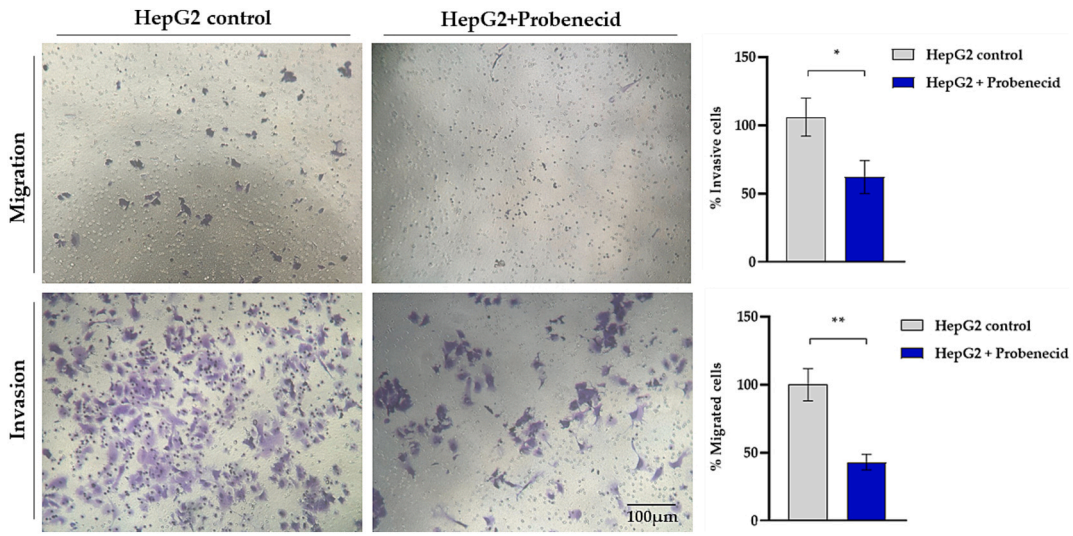

Fig. 3. Migration and invasion of HepG2 cells treated with Probenecid. Transwell assays assessed migration and Matrigel invasion of control and PBN-treated HepG2 cells. Migrating and invaded cells stained with crystal violet are shown in purple (magnification × 20, FLoidTM Cell Imaging Station). Data are presented as mean ± SEM from three independent experiments. Statistical significance was determined using Student's *t*-test; *p < 0.05, **p < 0.01.

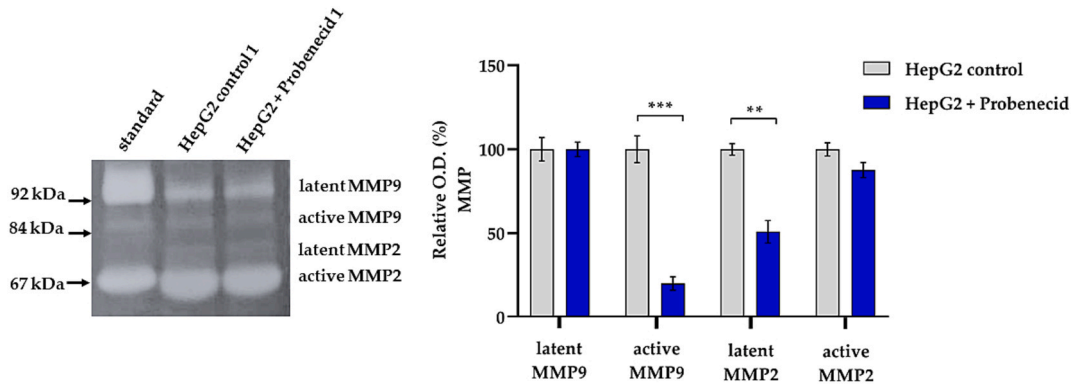

Fig. 4. MMP2 and MMP9 activity in culture media of HepG2 cells treated with Probenecid. Representative zymography gel (grayscale; white bands on black background) showing MMP2 and MMP9 activity, between control and PBN-treated HepG2 cells. A standard corresponding to a mix of purified MMP-2 and MMP-9 was included. Densitometric analysis of the bands was conducted across three independent experiments, with optical density (O.D.) normalized to total activity and expressed relative to control cells (set at 100 %). Data are presented as mean ± SEM from three independent replicates. Statistical significance was assessed using Student's *t*-test; **p < 0.01, ***p < 0.001.

by SDS-PAGE and transferred to nitrocellulose membranes (Amersham, Thermo Fisher Scientific, Waltham, MA, USA). Membranes were blocked in 5 % non-fat dry milk and incubated with primary antibodies overnight at 4 °C, followed by HRP-conjugated secondary antibodies. Blots were developed using chemiluminescence, and experiments were repeated in biological triplicates.

2.4. Cell adhesion assay

Samples were prepared as previously reported [18]. Briefly, PBN-treated and control cells (5×10^6 cells/mL) were stained with 5 µM Calcein AM (Thermo Fisher Scientific, Waltham, MA, USA) in serum-free medium for 30 min at 37 °C. After washing, cells were resuspended and seeded (100 µL/well) onto Matrigel-coated plates (100 µg/mL, Corning Life Sciences, Shanghai, China). After a 2-hour incubation, non-adherent cells were removed by PBS washes. Fluorescence of adherent cells was measured at 520 nm and adhesion was expressed as a percentage of the total initial fluorescence.

2.5. Migration and invasion assays

For migration assays, 2×10^5 serum-starved cells were seeded into the upper chamber of uncoated transwell inserts (8 µm pore size, 24-well format, Sterlitech, Auburn, WA, USA). For invasion assays, transwells were pre-coated with 100 µg/mL Matrigel. DMEM containing 10 % FBS was added to the lower chamber. After 48 h, cells remaining on the upper side were removed while migrated/invaded cells on the lower membrane surface were fixed in 4 % paraformaldehyde, stained with 0.1 % crystal violet and imaged under light microscopy. Quantification was performed using ImageJ software (NIH, Bethesda, MD, USA). Experiments were conducted in triplicate, and data are presented as mean ± SEM.

2.6. SDS–gelatin gel zymogram

Serum-free conditioned media from control and PBN-treated cells (50 µg protein) were mixed with non-reducing loading buffer and separated on 8 % SDS-PAGE gels containing 1 mg/mL gelatin (Sigma-Aldrich, St. Louis, MO, USA). Following electrophoresis, gels were washed twice in 2.5 % Triton X-100 (Sigma-Aldrich, St. Louis, MO, USA)

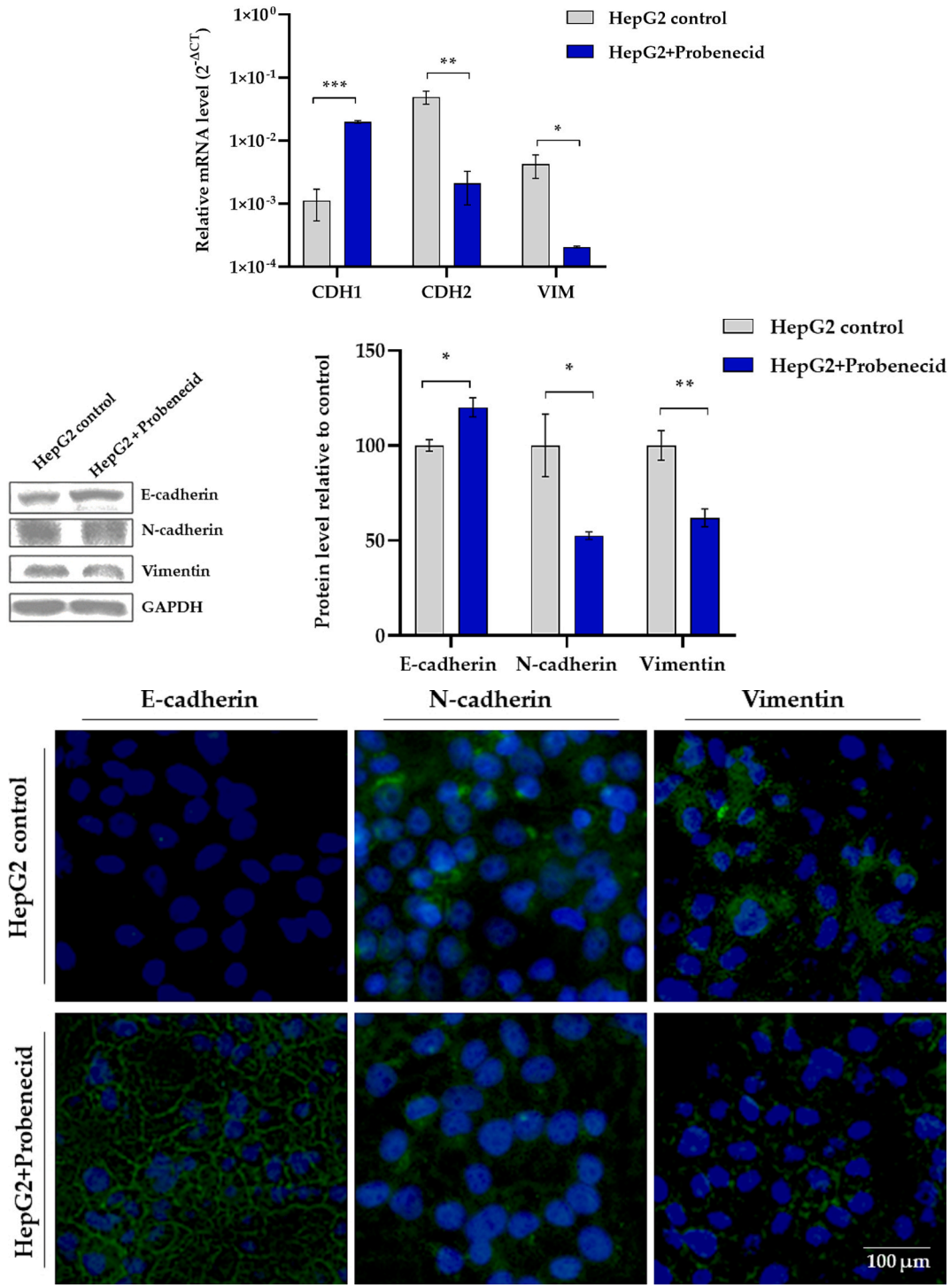

Fig. 5. Expression of EMT-related proteins in HepG2 cells treated with Probenecid. (a) Relative mRNA levels of E-cadherin, N-cadherin, and vimentin were quantified by RT-qPCR, normalized to β-actin, and expressed as $2^{-\Delta Ct}$. Data represent the mean ± SEM from at least three independent experiments. (b) Representative Western blot analysis of EMT proteins, with densitometric quantification of bands normalized to GAPDH. Protein levels are shown as percentages relative to control cells (set at 100 %), with data presented as mean ± SEM from three independent experiments. (c) Representative immunofluorescence images of E-cadherin, N-cadherin, and vimentin (green) in HepG2 cells treated with PBN or controls. Nuclei were counterstained with DAPI (blue). Images were captured using a 20 × FLoidTM Cell Imaging Station; scale bar: 100 µm. Statistical significance was determined using Student's *t*-test; *$p < 0.05$, **$p < 0.01$.

and incubated overnight at 37 °C in activation buffer (50 mM Tris–HCl, pH 6.8, 10 mM $CaCl_2$, 1 % Triton X-100). Gels were stained with Coomassie Brilliant Blue R-250 and G-250 (Sigma-Aldrich, St. Louis, MO, USA) and clear bands indicating MMPs activity were quantified densitometrically. As molecular weight and activity references, a mix of purified, active recombinant human MMP-2 and MMP-9 was loaded alongside the samples (PF023 and PF024, Sigma-Aldrich, St. Louis, MO, USA) corresponding to gelatinolytic bands of known size and activity. Serum samples (30 µg protein) from the xenograft mouse models were processed similarly.

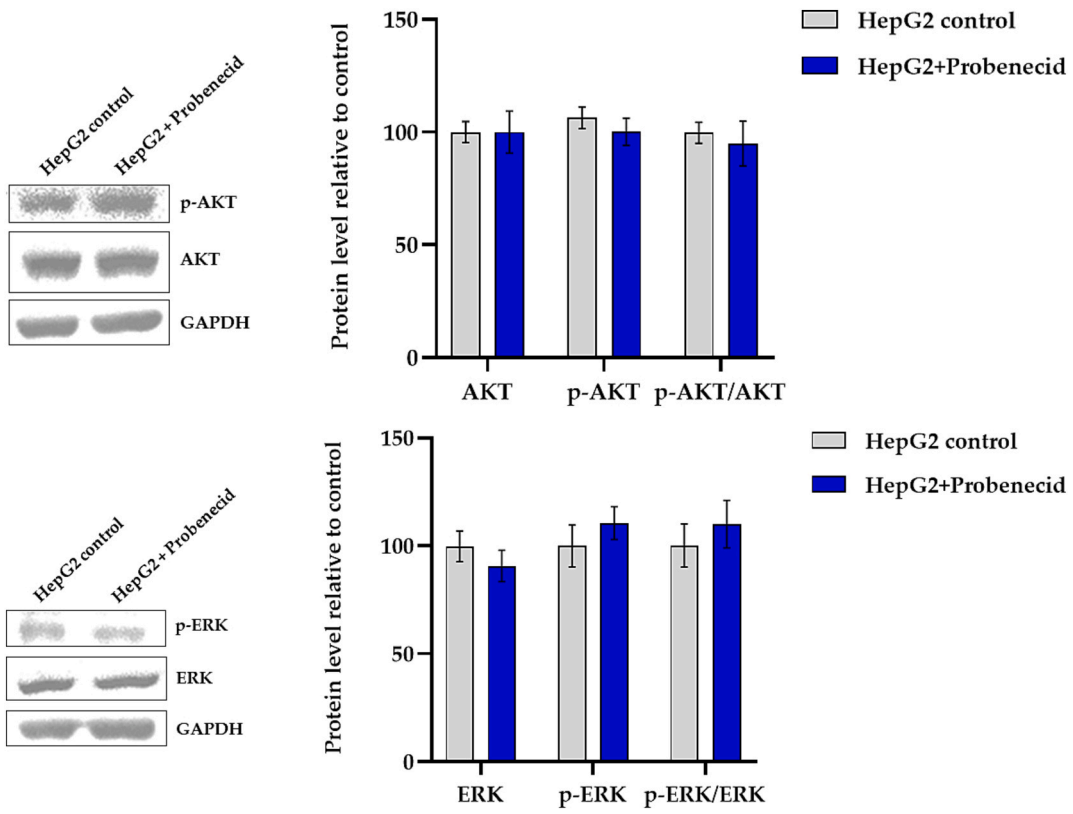

Fig. 6. Effects of Probenecid on AKT and ERK signaling pathways in HepG2 cells. (a) The ratio of phosphorylated to total AKT was assessed by densitometric analysis of immunoreactive bands detected with specific antibodies. Protein levels were normalized to GAPDH and expressed relative to control cells (set at 100 %). (b) The phosphorylated-to-total ERK ratio was similarly determined and normalized to GAPDH. Data are presented as mean ± SEM from three independent experiments.

2.7. Xenograft tumor model

Animal experiments were performed at the Good Laboratory Practices (GLP) Test facility of Biogem S.c.ar.l. (Ariano Irpino, Italy). Procedures were approved by the Ethics Committee (Protocol number 68/2019-PR, date of release 28/01/2019) at Biogem Animal House (Via Camporeale, 83,031 Ariano Irpino, Italy) following the National Academy of Sciences Guidelines.

Hepatocarcinoma cells expressing luciferase (HepG2-luc) were injected into 16 female CD1-nude mice at a concentration of 2×10^6 cells/50 µL. Tumor growth was monitored weekly by bioluminescence imaging (IVIS Spectrum; PerkinElmer, Waltham, MA, USA) following intraperitoneal injection (IP) of D-luciferin potassium salt (100 µL/10 g, PerkinElmer, Waltham, MA, USA). Imaging was performed 30 min post-injection under isoflurane anesthesia. Mice were then randomly divided into two experimental groups and treatments with PBN or vehicle (PBS; Thermo Fisher Scientific, Waltham, MA, USA) were administered IP every two days at a volume of 5 mL/kg. The 50 mg/kg dose of PBN was chosen according to Copsel et al. [11] who demonstrated effective inhibition of MRP transporters and tumor growth at this concentration in a mouse xenograft model, with no apparent toxicity.

Tumor radiance was recorded for up to 62 days. Tumor volume was measured as bioluminescence imaging (BLI) in terms of average radiance, representing photon flux (photons/sec/cm^2/sr) over the region of interest (ROI). A maximum average radiance of 1×10^8 photons/sec/cm^2/sr was set as the humane endpoint. Mice were sacrificed on day 67 for blood and tissue collection. Statistical analysis was performed using the Mann-Whitney *U* test (GraphPad Prism 6.0, San Diego, CA, USA).

2.8. ELISA for VEGF detection

Plasma levels of VEGF were measured using a commercial mouse VEGF ELISA kit (Proteintech, Rosemont, IL, USA) following the manufacturer's protocol. Absorbance was read at 450 nm using a GloMax Multi-Detection System (Promega, WI, USA) and VEGF concentrations were calculated from a standard curve.

2.9. Statistical analysis

All data are presented as mean ± standard error of the mean (SEM) from at least three independent biological replicates. Statistical significance was assessed using Student's *t*-test for comparisons between two groups or one-way ANOVA followed by Holm–Sidak post hoc test for multiple comparisons. In vivo tumor growth data were analyzed using non-parametric Mann–Whitney *U* test. A significance level of $\alpha = 0.05$ was used to determine statistical significance ($p < 0.05$, *$p < 0.01$, **$p < 0.001$). All statistical analyses were performed using GraphPad Prism version 6.0 (GraphPad Software, San Diego, CA, USA).

3. Results

3.1. PBN modulates purinergic receptor expression and cell-matrix dynamics

To clarify the impact of the treatment of HepG2 cells with PBN, we evaluated the expression level of key purinergic receptors involved in hepatocarcinoma signaling. As shown in Fig. 1, PBN decreased the expression of P2RY14, ADORA2A and ADORA3 compared with untreated controls. These receptors are key components of the purinergic network and have been implicated in tumor cell proliferation, motility and immune evasion [19–22]. The coordinated downregulation of these receptors by PBN suggests a suppression of both ATP- and ADO-dependent signaling routes that drive HCC aggressiveness. These findings provide initial evidence that PBN attenuates the purinergic

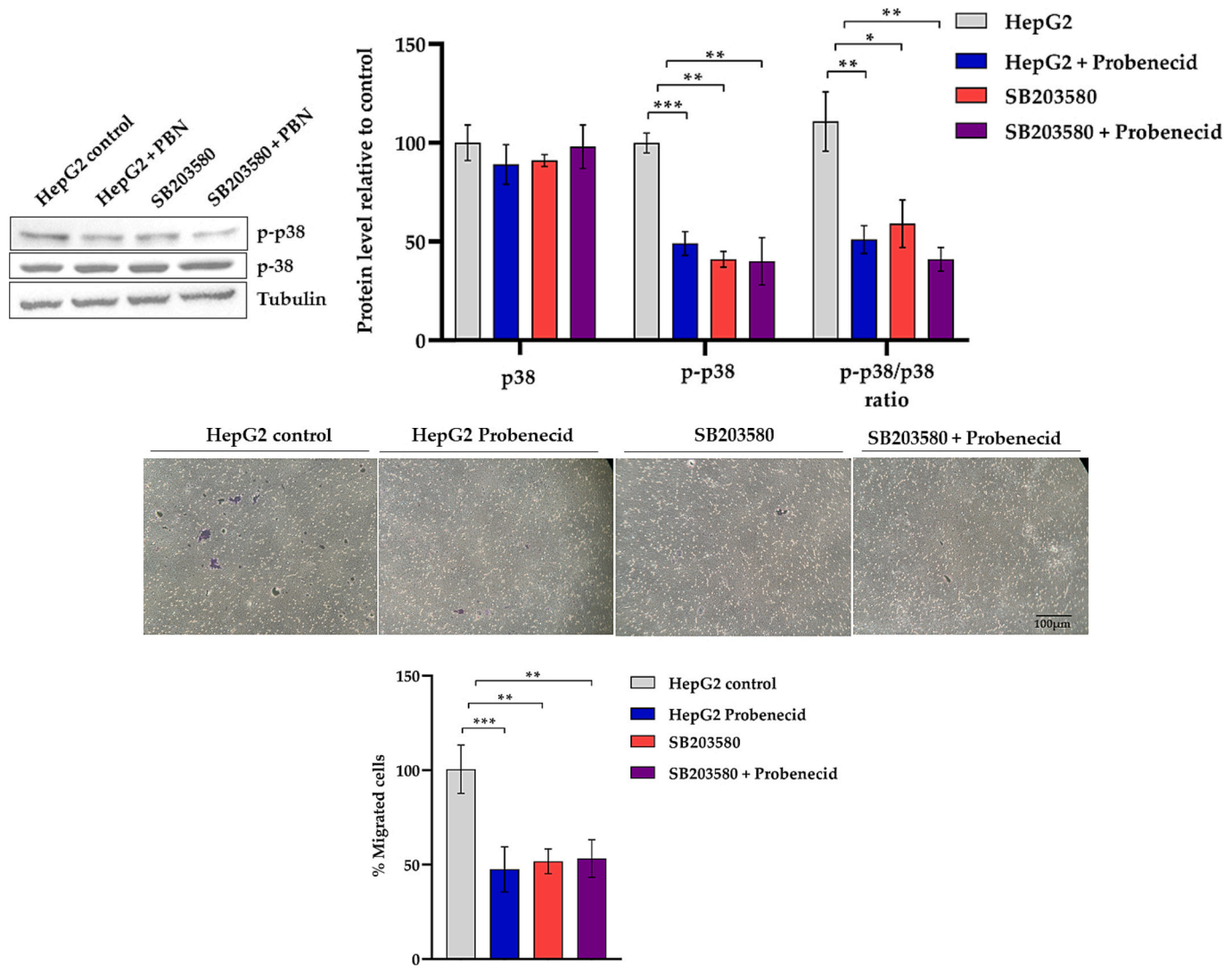

Fig. 7. Involvement of p38 MAPK in the antimigratory effect of Probenecid. (a) Western blot analysis of phosphorylated p38 (p-p38) and total p38 in HepG2 cells treated with PBN (250 μM), SB203580 (10 μM) or the combination of both. Densitometric quantification of p-p38/total p38 ratios is shown, with protein levels normalized to tubulin and expressed relative to control (set at 100 %). (b) Representative images of migrated HepG2 cells in transwell assays after 48 h of treatment with PBN, SB203580 or the combined treatment. Migrating cells stained with crystal violet are shown in purple (magnification × 20, FLoidTM Cell Imaging Station). Quantification of migrated cells is reported as percentage relative to control (set at 100 %). Data represent mean ± SEM from at least three independent experiments. Statistical analysis was performed using one-way ANOVA with Holm–Sidak correction; *p < 0.05, **p < 0.01, ***p < 0.001.

signaling cascade underlying migration and invasion in HepG2 cells.

PBN treatment significantly increased HepG2 cell adhesion to ECM-like Matrigel, doubling adhesion levels compared to controls (Fig. 2a). This effect was reversed by the addition of extracellular ATP or ADO, suggesting their involvement in regulating cell adhesion, likely through purinergic signaling.

To dissect the role of ATP-derived ADO in this process, we inhibited CD73 activity using AOPCP, a selective CD73 inhibitor. AOPCP abrogated the anti-adhesive effect of ADO, maintaining high adhesion levels similar to those observed in PBN-treated cells (Fig. 2b), indicating that CD73 activity is required for ADO-mediated reduction of adhesion. Furthermore, PBN treatment led to an upregulation of ITGA2 and ITGB1 expression, key genes for cell-ECM interactions (Fig. 2c).

3.1.1. *PBN inhibits cell invasion and selectively modulates MMPs activity*

Transwell assays demonstrated that PBN significantly reduced both migration and invasion of HepG2 cells (Fig. 3).

To investigate the mechanisms underlying this effect, we performed gelatin zymography to assess matrix metalloproteinase activity. PBN selectively decreased the activity of MMP9, a key enzyme involved in ECM degradation, while MMP2 activity remained unaffected (Fig. 4). This suggests that the anti-invasive effect of PBN may be mediated through the selective inhibition of MMP9.

3.1.2. *PBN modulates EMT markers expression*

PBN treatment led to an increased expression of E-cadherin, an epithelial marker associated with reduced migratory and invasive potential, and a decreased expression of the mesenchymal markers vimentin and N-cadherin, which are typically linked to enhanced cell motility and aggressiveness (Fig. 5). These results indicate that PBN may suppress EMT and thereby limit the metastatic potential of HepG2 cells.

3.2. *PBN inhibits migration through p38 MAPK signaling*

To investigate the signaling pathways underlying the effects of PBN on cell motility, we first examined AKT and ERK activation. PBN did not modify the phosphorylation of either protein (Fig. 6a,b), indicating that these pathways are not involved in the reduction of cell motility.

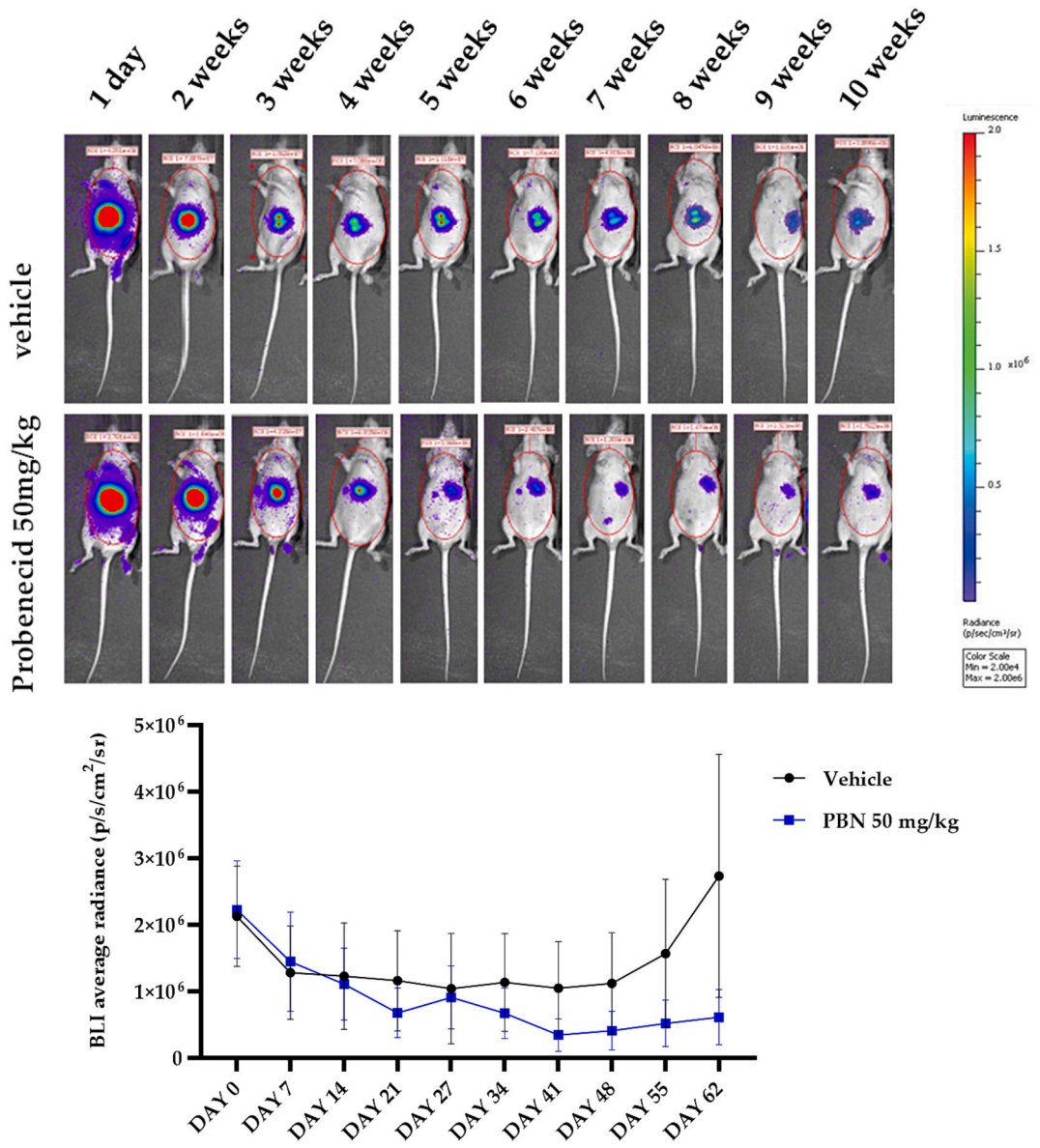

Fig. 8. In vivo effects of PBN in an orthotopic HCC mouse model. (a) IVIS imaging of tumor progression in eight mice per group from day 0 (treatment initiation) today 62 (end of treatment). (b) Mean tumor bioluminescence over the experimental period. Statistical analysis was performed using two-way ANOVA with Šidák's multiple comparisons test; no statistically significant differences were observed between groups (P = 0.39).

We then assessed p38 MAPK and observed that PBN markedly decreased p-p38 levels (Fig. 7a). To validate the functional relevance of this pathway, HepG2 cells were treated with the selective p38 inhibitor SB203580, alone or in combination with PBN. As shown in Fig. 7a, both PBN and SB203580 reduced p-p38 without affecting total p38 and the co-treatment produced a comparable decrease.

Consistent with the biochemical data, SB203580 significantly inhibited cell migration to a similar extent as PBN (Fig. 7b). The combined treatment did not further reduce migration, supporting the hypothesis that both agents act on the same signaling axis. Overall, these findings indicate that the antimigratory effect of PBN is mediated through inhibition of the p38 MAPK pathway.

3.3. PBN reduces tumor growth and angiogenesis in an orthotopic HCC mouse model

Importantly, PBN treatment did not induce systemic toxicity, as body weight of mice remained comparable between groups throughout the study period. In an orthotopic mouse model of HCC, bioluminescence imaging demonstrated a 78 % decrease in tumor signal intensity in mice treated with PBN (50 mg/kg, i.p. every two days) after 62 days relative to vehicle-treated controls. Although the difference was not statistically significant (P = 0.39), this trend may indicate a potential role of PBN in suppressing tumor engraftment (Fig. 8).

To evaluate angiogenic activity, plasma levels of VEGF were measured by ELISA and found to be significantly reduced in the PBN-treated group, suggesting that PBN may influence angiogenesis and tumor engraftment (Fig. 9a). Additionally, zymography of plasma samples revealed decreased activity of both the latent and active forms of MMP9 and MMP2 (Fig. 9b), supporting a role for PBN in limiting both angiogenesis and extracellular matrix remodeling *in vivo*.

4. Discussion

Previous studies have shown that PBN, a well-established drug used to treat gout, reduces extracellular ATP levels in HepG2 cells, also through the inhibition of ABCC6, a membrane transporter involved in ATP efflux and highly expressed in these cells [8,14]. PBN has also been

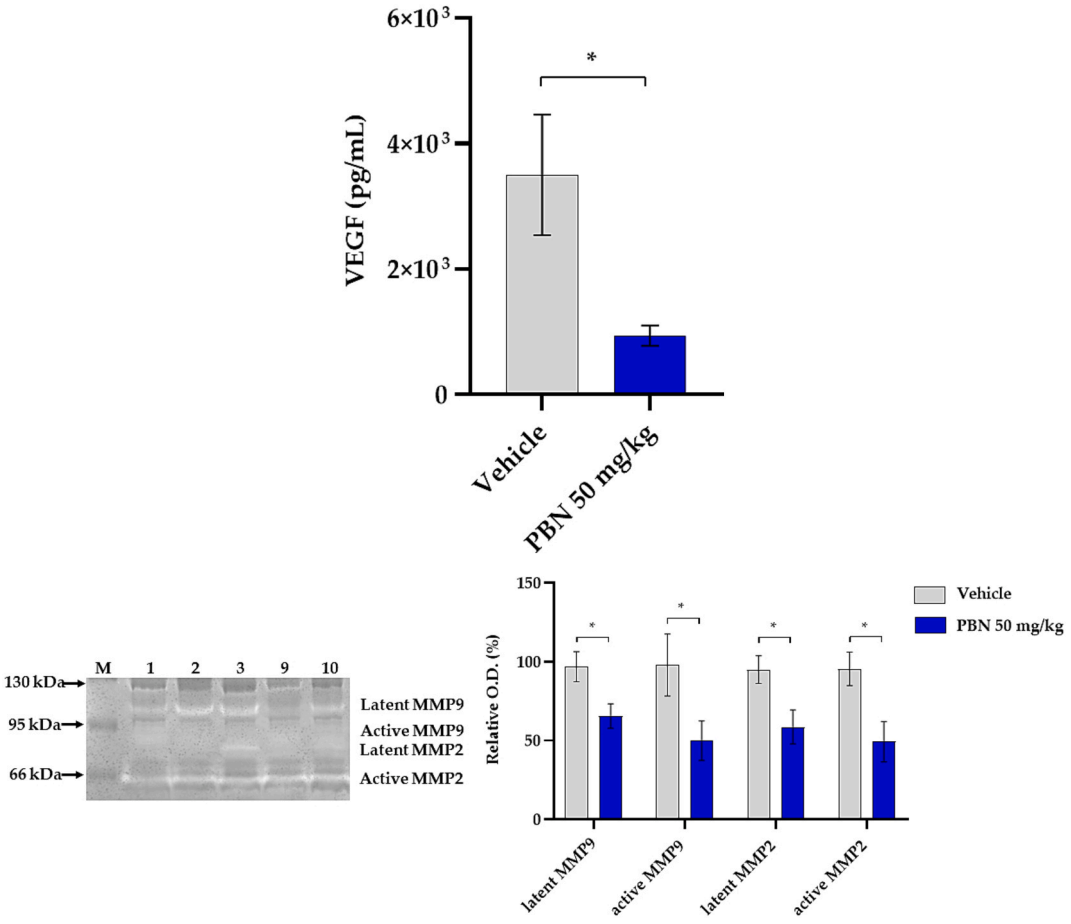

Fig. 9. Plasma VEGF levels and MMP2 and MMP9 activity in plasma from mice treated with PBN. (a) VEGF concentrations in plasma were measured by sandwich ELISA in an orthotopic liver cancer mouse model treated with PBN (50 mg/kg) or vehicle. (b) Representative gelatin zymography gel (grayscale; white bands on a black background) showing MMP2 and MMP9 activity, along with densitometric analysis of band intensities. "M" indicates molecular weight markers. Lanes 1, 2 and 3 correspond to plasma samples from three tumor-bearing mice treated with vehicle. Lanes 9, 10 and 11 correspond to plasma samples from three tumor-bearing mice treated with PBN. Optical density (O.D.) was normalized to total proteolytic activity and expressed relative to vehicle-treated controls (set to 100 %). Data are presented as mean ± SEM. Statistical analysis was conducted using Student's *t*-test; *p < 0.05, **p < 0.01.

reported to downregulate CD73, an ectonucleotidase that hydrolyzes extracellular ATP to ADO [17,23], suggesting a dual modulatory effect on purinergic signaling in this cell model.

Given the central role of ATP and ADO in the tumor microenvironment, we investigated the mechanisms underlying the increased adhesion and reduced migration and invasiveness of HCC cells treated with PBN.

As shown in Fig. 1, PBN downregulated key purinergic receptors, including P2RY14, ADORA2A, and ADORA3, which are involved in signaling pathways such as ERK/MAPK and PI3K/AKT that regulate EMT, angiogenesis, invasion and cytoskeletal remodeling [20,21,24,25]. The selective modulation of these receptors may impair tumor-promoting signaling and adaptive survival mechanisms.

Enhanced cell adhesion to ECM components in PBN-treated cells was associated with upregulation of integrins ITGA2 and ITGB1 (Fig. 2), well-characterized mediators of cell–matrix interactions that help maintain epithelial traits and limit cell motility [26–30]. This effect was reversed by the addition of extracellular ATP or ADO, suggesting that purinergic signaling plays a regulates integrin-dependent adhesion dynamics [31]. Furthermore, the ability of AOPCP, a selective CD73 inhibitor, to reverse the anti-adhesive effect of ADO highlights the central role of CD73-generated extracellular ADO in controlling cell–matrix interactions. Although ATP levels were previously shown to be reduced in the extracellular environment of PBN-treated HepG2 cells [14], the AOPCP data emphasize the functional importance of the downstream hydrolysis product, ADO, in this process. These findings align with existing literature suggesting that ADO modulates integrin-mediated adhesion and contributes to a more epithelial, less migratory phenotype in tumor cells [22,32,33].

Consistent with these observations, PBN significantly reduced both migration and invasion in transwell assays (Fig. 3). These functional effects align with the molecular changes reported in Figs. 1–2, suggesting that inhibition of purinergic signaling and upregulation of adhesion-related integrins collectively result in impaired motility.

The decrease in invasiveness was associated with selective inhibition of MMP9 activity, while MMP2 remained unaffected, indicating a specific modulation of ECM-degrading proteases involved in metastatic dissemination (Fig. 4). Given the established role of MMP9 in promoting extracellular matrix breakdown and facilitating cell migration [34,35], its inhibition likely contributes directly to the reduced invasive behavior observed in PBN-treated cells.

The effects of PBN on EMT markers were also consistent with these findings. PBN increased the expression of the epithelial marker E-cadherin while decreasing mesenchymal markers N-cadherin and vimentin (Fig. 5), indicating suppression of EMT [36,37], This molecular shift toward an epithelial phenotype is consistent with the reduced migratory and invasive behavior observed in treated cells.

To identify the signaling pathways involved, we examined AKT, ERK and p38 MAPK phosphorylation (Fig. 6). While AKT and ERK activation remained unchanged (Figs. 6a,b), PBN decreased phosphorylation of

p38 MAPK (Fig. 7a), suggesting that this pathway mediates the observed phenotypic effects. Since that p38 MAPK has been implicated in cytoskeletal dynamics and metastatic behavior [38], its inhibition provides a plausible molecular explanation for the reduction in cell motility and EMT markers. Consistent with these results, pharmacological inhibition of p38 MAPK using SB203580 reproduced the antimigratory effects of PBN, providing functional validation of the pathway involved. SB203580 reduced migration to an extent comparable to PBN and the absence of additive effects in the combined treatment indicates convergence on the same signaling cascade (Fig. 7 b). Western blot analysis further confirmed that both treatments effectively suppressed p38 phosphorylation (Fig. 7a). These findings strongly support the conclusion that inhibition of p38 MAPK signaling is a key mechanism by which PBN reduces cell migration and contributes to EMT suppression in HepG2 cells.

The *in vivo* findings support the *in vitro* results. In an orthotopic HCC mouse model (Fig. 8), PBN treatment showed a trend toward reduced tumor radiance compared with controls. Although the difference was not statistically significant and control tumors displayed unexpected signal fluctuations likely reflecting biological heterogeneity in tumor engraftment efficiency and technical factors inherent to the orthotopic model and bioluminescence imaging, the overall pattern suggests a potential moderating effect of PBN on tumor growth. The lack of statistical significance indicates that these *in vivo* findings should be interpreted with caution and that further studies with extended treatment durations that are ethically permissible are warranted.

Moreover, PBN-treated mice exhibited lower plasma VEGF levels and reduced MMP2 and MMP9 activities (Fig. 9), suggesting inhibition of angiogenesis and ECM remodeling *in vivo*. Given that MMP-dependent matrix degradation facilitates VEGF activation and endothelial receptor exposure [39–41], the concurrent downregulation of VEGF and MMP activity indicates that PBN may interfere with this MMP–VEGF signaling axis. Such interference would limit neovascularization and weaken the vascular support required for tumor engraftment and growth. Although the available plasma biomarkers consistently support an anti-angiogenic response, future preclinical studies incorporating direct tissue-based analyses of tumor vasculature will be needed to fully validate the *in vivo* anti-angiogenic effects of Probenecid.

The effects of PBN observed in this study using HepG2 cells, a well-established HCC model with robust purinergic signaling and high ABC transporter expression, are consistent with previous reports in other tumor models [11,12,15]. While our results highlight the relevance of extracellular nucleotide regulation in hepatocellular carcinoma, validation in additional HCC cell lines and *in vivo* models will still be required.

In conclusion, PBN appears to exert antitumor-related biological effects in HepG2 cells by modulating purinergic signaling, enhancing integrin-mediated adhesion, inhibiting EMT and suppressing angiogenesis, supporting its potential as a therapeutic agent for HCC and encouraging further preclinical and clinical investigation.

CRediT authorship contribution statement

Ilenia Matera: Visualization, Investigation, Formal analysis. **Alessandro Pistone:** Investigation. **Maria Antonietta Castiglione Morelli:** Writing – review & editing. **Faustino Bisaccia:** Writing – original draft, Resources. **Angela Ostuni:** Writing – review & editing, Writing – original draft, Project administration, Conceptualization.

Funding

This research did not receive any specific grant from funding agencies in the public, commercial, or not-for-profit sectors.

Declaration of competing interest

The authors declare that they have no known competing financial interests or personal relationships that could have appeared to influence the work reported in this paper.

Data availability

Data will be made available on request.

References

[1] J.M. Llovet, R.K. Kelley, A. Villanueva, A.G. Singal, E. Pikarsky, S. Roayaie, R. Lencioni, K. Koike, J. Zucman-Rossi, R.S. Finn, Hepatocellular carcinoma, Nat. Rev. Dis. Primers 7 (2021) 1–28, https://doi.org/10.1038/s41572-020-00240-3.
[2] M.A. Hijazi, A. Gessner, N. El-Najjar, Repurposing of chronically used drugs in cancer therapy: a chance to grasp, Cancers (Basel) 15 (2023) 3199, https://doi.org/10.3390/cancers15123199.
[3] Y. Xia, M. Sun, H. Huang, W.-L. Jin, Drug repurposing for cancer therapy, Signal Transduct. Target. Ther. 9 (2024) 92, https://doi.org/10.1038/s41392-024-01808-1.
[4] G. Burnstock, Purine and purinergic receptors, Brain Neurosci. Adv. 2 (2018) 2398212818817494, https://doi.org/10.1177/2398212818817494.
[5] F. Di Virgilio, V. Vultaggio-Poma, M. Tarantini, A.L. Giuliani, Overview of the role of purinergic signaling and insights into its role in cancer therapy, Pharmacol. Ther. 262 (2024) 108700, https://doi.org/10.1016/j.pharmthera.2024.108700.
[6] V. Vultaggio-Poma, A.C. Sarti, F. Di Virgilio, Extracellular ATP: a feasible target for cancer therapy, Cells 9 (2020) 2496, https://doi.org/10.3390/cells9112496.
[7] D. Khanna, J.D. Fitzgerald, P.P. Khanna, S. Bae, M.K. Singh, T. Neogi, M. H. Pillinger, J. Merill, S. Lee, S. Prakash, et al., 2012 American college of rheumatology guidelines for management of Gout. part 1: systematic nonpharmacologic and pharmacologic therapeutic approaches to hyperuricemia, Arthritis Care Res. 64 (2012) 1431–1446, https://doi.org/10.1002/acr.21772.
[8] F. Bisaccia, P. Koshal, V. Abruzzese, M.A.C. Morelli, A. Ostuni, Structural and functional characterization of the ABCC6 transporter in hepatic cells: role on PXE, cancer therapy and drug resistance, Int. J. Mol. Sci. 22 (2021) 2858, https://doi.org/10.3390/ijms22062858.
[9] S.K. Nigam, K.T. Bush, G. Martovetsky, S.-Y. Ahn, H.C. Liu, E. Richard, V. Bhatnagar, W. Wu, The organic anion transporter (OAT) family: a systems biology perspective, Physiol. Rev. 95 (2015) 83–123, https://doi.org/10.1152/physrev.00025.2013.
[10] M. Koval, W.J. Schug, B.E. Isakson, Pharmacology of pannexin channels, Curr. Opin. Pharmacol. 69 (2023) 102359, https://doi.org/10.1016/j.coph.2023.102359.
[11] S. Copsel, A. Bruzzone, M. May, J. Beyrath, V. Wargon, J. Cany, F.G.M. Russel, C. Shayo, C. Davio, Multidrug resistance protein 4/ATP binding cassette transporter 4: a new potential therapeutic target for acute myeloid leukemia, Oncotarget 5 (2014) 9308–9321, https://doi.org/10.18632/oncotarget.2425.
[12] J. Uwada, S. Mukai, N. Terada, H. Nakazawa, M.S. Islam, T. Nagai, M. Fujii, K. Yamasaki, T. Taniguchi, T. Kamoto, et al., Pleiotropic effects of probenecid on three-dimensional cultures of prostate cancer cells, Life Sci. 278 (2021) 119554, https://doi.org/10.1016/j.lfs.2021.119554.
[13] C.-A. D'Alessandro, J.C. Martínez-Lorente, J. Montoya-Zorrilla, Probenecid is a chemosensitizer in cancer cell lines, Cancer Chemother. Pharmacol. 69 (2012) 1013–1021, https://doi.org/10.1007/s00280-011-1725-6.
[14] A. Ostuni, M. Carmosino, R. Miglionico, V. Abruzzese, F. Martinelli, D. Russo, I. Laurenzana, A. Petillo, F. Bisaccia, Inhibition of ABCC6 transporter modifies cytoskeleton and reduces motility of HepG2 cells via purinergic pathway, Cells 9 (2020) 1410, https://doi.org/10.3390/cells9061410.
[15] V. Abruzzese, C.H.C. Sukowati, C. Tiribelli, I. Matera, A. Ostuni, F. Bisaccia, The expression level of ABCC6 transporter in colon cancer cells correlates with the activation of different intracellular signaling pathways, Pathophysiology 29 (2022) 173–186, https://doi.org/10.3390/pathophysiology29020015.
[16] Abruzzese, V.; Matera, I.; Martinelli, F.; Carmosino, M.; Koshal, P.; Milella, L.; Bisaccia, F.; Ostuni, A. Effect of Quercetin on ABCC6 Transporter: Implication in HepG2 Migration. *International journal of molecular sciences* **2021**, *22*, doi:10.3390/ijms22083871.
[17] F. Martinelli, F. Cuviello, M.C. Pace, M.F. Armentano, R. Miglionico, A. Ostuni, F. Bisaccia, Extracellular ATP regulates CD73 and ABCC6 expression in HepG2 cells, Front. Mol. Biosci. 5 (2018) 75, https://doi.org/10.3389/fmolb.2018.00075.
[18] I. Matera, R. Miglionico, V. Abruzzese, G. Marchese, G.M. Ventola, M. A. Castiglione Morelli, F. Bisaccia, A. Ostuni, A regulator role for the ATP-binding cassette subfamily C member 6 transporter in HepG2 Cells: effect on the dynamics of cell–cell and cell–matrix interactions, Int. J. Mol. Sci. 24 (2023) 16391, https://doi.org/10.3390/ijms242216391.
[19] K. Shah, S.A. Moharram, J.U. Kazi, Acute leukemia cells resistant to PI3K/mTOR inhibition display upregulation of P2RY14 expression, Clin. Epigenetics 10 (2018) 83, https://doi.org/10.1186/s13148-018-0516-x.
[20] T. Xu, S. Xu, Y. Yao, X. Chen, Q. Zhang, X. Zhao, X. Wang, J. Zhu, N. Liu, J. Zhang, et al., P2RY14 downregulation in lung adenocarcinoma: a potential therapeutic target associated with immune infiltration, J. Thorac. Dis. 14 (2022) 515–535, https://doi.org/10.21037/jtd-22-115.

[21] L. Ran, X. Mou, Z. Peng, X. Li, M. Li, D. Xu, Z. Yang, X. Sun, T. Yin, ADORA2A promotes proliferation and inhibits apoptosis through PI3K/AKT pathway activation in colorectal carcinoma, Sci. Rep. 13 (2023) 19477, https://doi.org/10.1038/s41598-023-46521-1.
[22] C. Mazziotta, J.C. Rotondo, C. Lanzillotti, G. Campione, F. Martini, M. Tognon, Cancer biology and molecular genetics of A3 adenosine receptor, Oncogene 41 (2022) 301–308, https://doi.org/10.1038/s41388-021-02090-z.
[23] Z. Gao, K. Dong, H. Zhang, The roles of CD73 in cancer, Biomed Res. Int. 2014 (2014) 460654, https://doi.org/10.1155/2014/460654.
[24] D. Draganov, P.P. Lee, Purinergic signaling within the tumor microenvironment, Adv. Exp. Med. Biol. 1270 (2021) 73–87, https://doi.org/10.1007/978-3-030-47189-7_5.
[25] P. Fishman, S.M. Stemmer, A. Bareket-Samish, M.H. Silverman, W.D. Kerns, Targeting the A3 adenosine receptor to treat hepatocellular carcinoma: anti-cancer and hepatoprotective effects, Purinergic Signal. 19 (2023) 513–522, https://doi.org/10.1007/s11302-023-09925-2.
[26] R. Wafai, E.D. Williams, E. de Souza, P.T. Simpson, A.E. McCart Reed, J. R. Kutasovic, M. Waltham, C.E. Snell, T. Blick, E.W. Thompson, et al., Integrin Alpha-2 and Beta-1 expression increases through multiple generations of the EDW01 patient-derived xenograft model of breast cancer—insight into their role in epithelial–mesenchymal transition in vivo gained from an in vitro model system, Breast Cancer Res. 22 (2020) 136, https://doi.org/10.1186/s13058-020-01366-8.
[27] S. Gou, A. Wu, Z. Luo, Integrins in cancer stem cells, Front. Cell Dev. Biol. 12 (2024) 1434378, https://doi.org/10.3389/fcell.2024.1434378.
[28] C. Rattanasinchai, P. Navasumrit, M. Ruchirawat, Elevated ITGA2 expression promotes collagen type I-induced clonogenic growth of intrahepatic cholangiocarcinoma, Sci. Rep. 12 (2022) 22429, https://doi.org/10.1038/s41598-022-26747-1.
[29] L. Sun, S. Guo, Y. Xie, Y. Yao, The characteristics and the multiple functions of integrin β1 in human cancers, J. Transl. Med. 21 (2023) 787, https://doi.org/10.1186/s12967-023-04696-1.
[30] H. Hamidi, J. Ivaska, Every step of the way: integrins in cancer progression and metastasis, Nat. Rev. Cancer 18 (2018) 533–548, https://doi.org/10.1038/s41568-018-0038-z.
[31] C.L. Alvarez, M.F. Troncoso, M.V. Espelt, Extracellular ATP and adenosine in tumor microenvironment: roles in epithelial–mesenchymal transition, cell migration, and invasion, J. Cell. Physiol. 237 (2022) 389–400, https://doi.org/10.1002/jcp.30580.
[32] Á. Torres, J.I. Erices, F. Sanchez, P. Ehrenfeld, L. Turchi, T. Virolle, D. Uribe, I. Niechi, C. Spichiger, J.D. Rocha, et al., Extracellular adenosine promotes cell migration/invasion of glioblastoma stem-like cells through A3 adenosine receptor activation under hypoxia, Cancer Lett. 446 (2019) 112–122, https://doi.org/10.1016/j.canlet.2019.01.004.
[33] D. Pietrobono, C. Giacomelli, L. Marchetti, C. Martini, M.L. Trincavelli, High adenosine extracellular levels induce glioblastoma aggressive traits modulating the mesenchymal stromal cell secretome, Int. J. Mol. Sci. 21 (2020) 7706, https://doi.org/10.3390/ijms21207706.
[34] D. Kalali, The role of the matrix metalloproteinase-9 gene in tumor development and metastasis: a narrative review, Glob. Med. Genet. 10 (2023) 48–53, https://doi.org/10.1055/s-0043-1768166.
[35] Z. Yuan, Y. Li, S. Zhang, X. Wang, H. Dou, X. Yu, Z. Zhang, S. Yang, M. Xiao, Extracellular matrix remodeling in tumor progression and immune escape: from mechanisms to treatments, Mol. Cancer 22 (2023) 1–42, https://doi.org/10.1186/s12943-023-01744-8.
[36] J. Fares, M.Y. Fares, H.H. Khachfe, H.A. Salhab, Y. Fares, Molecular principles of metastasis: a hallmark of cancer revisited, Signal Transduct. Target. Ther. 5 (2020) 1–17, https://doi.org/10.1038/s41392-020-0134-x.
[37] W. Lu, Y. Kang, Epithelial–mesenchymal plasticity in cancer progression and metastasis, Dev. Cell 49 (2019) 361–374, https://doi.org/10.1016/j.devcel.2019.04.010.
[38] S. Kudaravalli, P. den Hollander, S.A. Mani, Role of P38 MAP kinase in cancer stem cells and metastasis, Oncogene 41 (2022) 3177–3185, https://doi.org/10.1038/s41388-022-02329-3.
[39] Y. Liu, H. Zhang, L. Yan, W. Du, M. Zhang, H. Chen, L. Zhang, G. Li, J. Li, Y. Dong, et al., MMP-2 and MMP-9 contribute to the angiogenic effect produced by hypoxia/15-HETE in pulmonary endothelial cells, J. Mol. Cell. Cardiol. 121 (2018) 36–50, https://doi.org/10.1016/j.yjmcc.2018.06.006.
[40] Azevedo Martins, J.M.; Rabelo-Santos, S.H.; do Amaral Westin, M.C.; Zeferino, L.C. Tumoral and Stromal Expression of MMP-2, MMP-9, MMP-14, TIMP-1, TIMP-2, and VEGF-A in Cervical Cancer Patient Survival: A Competing Risk Analysis. *BMC Cancer* **2020**, *20*, 660, doi:10.1186/s12885-020-07150-3.
[41] E.I. Deryugina, J.P. Quigley, Tumor angiogenesis: MMP-mediated induction of intravasation- and metastasis-sustaining neovasculature, Matrix Biol. 44–46 (2015) 94–112, https://doi.org/10.1016/j.matbio.2015.04.004.